Journal of the Brazilian Society of Mechanical Sciences and Engineering (2019) 41:469
https://doi.org/10.1007/s40430-019-1986-2

TECHNICAL PAPER

ZrB_2 nanoparticles transmuting tribological properties of Al_3Zr/AA5052 composite

Gaurav Gautam[1] · Narendra Kumar[2] · Anita Mohan[3] · Sunil Mohan[4] · Devendra Singh[1]

Received: 20 September 2018 / Accepted: 27 September 2019 / Published online: 3 October 2019

Abstract
Good work hardenability, moderate to high strength of AA5052 alloy and high melting point and elastic modulus of Al_3Zr with limited wear resistance have been the driving force to transmute Al_3Zr/AA5052 composite by generations of ZrB_2 nanoparticles. For this purpose, the varying amounts of ZrB_2 particles in Al_3Zr/AA5052 composite have been produced by direct melt reaction in situ technique. The phase identification, microstructural studies and wear testing have been performed for all the composites. The phase identification and microstructural studies indicate that the ZrB_2 particles are formed successfully in the Al_3Zr/AA5052Al composite with hexagonal and rectangular morphology within a size range of 10–190 nm. Wear testing results show that friction coefficient (COF) fluctuates with sliding distance, whereas it decreases with normal load. For the composite without ZrB_2, the COF is exhibited increasing trend with sliding velocity, while for the hybrid composites initially it decreases, but beyond 2 m/s sliding velocities it starts increasing. Wear studies also show that with ZrB_2 generation in Al_3Zr/AA5052 composites can be used up to larger loads and higher sliding velocities while being in mild wear regime. It is observed that the mild wear regime extends and COF increases with the increase in vol% of ZrB_2 particles. Texture analysis of worn surfaces is in agreement with the results. The present investigation shows that in situ (ZrB_2 + Al_3Zr)/AA5052 hybrid composites could be a promising material in the applications requiring high wear resistance and high COF such as braking system.

Keywords Aluminium matrix composites (AMCs) · Wear · Friction · Texture analysis

1 Introduction

Particulate-reinforced aluminium matrix composites (PRAMCs) have wide applications in automobiles and railway vehicles parts due to their superior tribological properties than un-reinforced alloys [1–3]. PRAMCs reinforced with single reinforcement generally exhibit marginal improvement in wear resistance as compared to base alloy [4, 5]. However, multiple particulate reinforcements in the PRAMCs improve wear resistance extensively. Different materials have been synthesized by multiple reinforcements with promising results [6–9], but the work is limited with Al_3Zr and ZrB_2 combination [1, 10–12]. The Al_3Zr exhibits low density, high melting point and high elastic modulus with excellent resistance to oxidation and corrosion [2]. However, ZrB_2 has high melting point, high strength and hardness, good thermal and electrical conductivity, strong covalent bonding and thermal shock resistance [3]. These could be potential reinforcements for the PRAMCs as a material for the tribological applications. PRAMCs are generally fabricated by ex situ or in situ processes, but the latter one is preferred by the researchers because these processes provide the advantages of finer size, clean interface and uniform distribution of the particles in the composite matrix. The direct melt reaction (DMR) which is one of the in situ processes is selected as a potential fabrication technique

Technical Editor: Fernando Antonio Forcellini, Dr.

✉ Gaurav Gautam
gauravgautamm1988@gmail.com

[1] Department of Metallurgical and Materials Engineering, IIT Roorkee, Roorkee, U.K. 247667, India

[2] Department of Mechanical Engineering, BIET, Jhansi, U.P. 284128, India

[3] Department of Physics, IIT (BHU), Varanasi, U.P. 221005, India

[4] Department of Metallurgical Engineering, IIT (BHU), Varanasi, U.P. 221005, India

due to its simplicity, low cost and near-net-shape forming capability [12].

The researchers have prepared different kinds of PRAMCs using different aluminium matrices and reinforcements [1, 4, 10, 11, 13–15], but the work on AA5052 alloy matrix is limited. This alloy exhibits the moderate to high strength, good work hardenability, good weldability and good resistance to corrosion in marine environments due to magnesium [2]. Therefore, AA5052 alloy has been selected in the present study as a matrix material.

Zhang et al. [1] and Zhang et al. [10] prepared the PRAMCs reinforced with Al_3Zr and ZrB_2 through magneto-chemistry and observed hexagonal and tetragonal in situ formed particles of ZrB_2 and Al_3Zr. They also observed decrease in mass loss during wear with increasing amount of particles. Zhao et al. [11] while studying effect of melt temperature on the morphologies of reinforcement particles noticed that morphology of Al_3Zr particles changes into fibre through changing from spherical, tetragon and rod with increasing melt temperature, while ZrB_2 particles did not show any visible change in morphology. They also observed minimum wear with spherical Al_3Zr particles.

Agarwal et al. [4] investigated the tribological performance of aluminium matrix composites reinforced with trialuminide (Al_3Fe) fabricated through powders of aluminium and iron. They found that wear rate decreased with Al_3Fe particles. It was due to the originating of mechanically mixed layer (MML), whereas coefficient of friction increased due to the increasing adhesion. With sliding velocity, wear rate decreased up to a certain sliding velocity, and after attaining a minimum value, it increased sharply. Similar observations have been made by different researchers in aluminium matrix composites [13, 14]. Dinaharan et al. [15] fabricated the ZrB_2/AA6061 composite by in situ reaction technique and observed spherical and elliptical ZrB_2 particles, and these in situ formed particles refined aluminium matrix. They also observed improvement in hardness, ultimate tensile strength with the incorporation of ZrB_2 particles. The wear properties also improved with the addition of ZrB_2 particles due to high hardness and grain refinement of matrix.

Previous work on synthesis and characterization of ($ZrB_2 + Al_3Zr$)/AA5052 hybrid composites has shown successful generation of multiple reinforcements in AA5052 alloy, namely Al_3Zr and ZrB_2 with improved mechanical properties. Different strengthening mechanisms were also estimated for these composites [12, 16, 17].

In the present work, tribological behaviour of the above-mentioned in situ ($ZrB_2 + Al_3Zr$)/AA5052 hybrid composites has been investigated. Composites have been subjected to dry sliding wear and friction tests at different combinations of normal loads and sliding velocities. Wear tracks and debris are analysed by SEM and EDS, and texture has been studied under profilometer to interpret the operative wear mechanisms.

2 Experimental details

2.1 Composite fabrication and microstructural analysis

The AA5052 alloy (Al–2.6 Mg–0.13 Si–0.3 Fe–0.18–Cr–0.1–Mn–0.01–Cu–0.05 Zn) ingot and potassium hexa-fluro-zirconate (K_2ZrF_6) and potassium tetra-fluro-borate (KBF_4) powders were selected as a starting material to fabricate the composites. The composites were fabrication by the direct melt reaction (DMR) in situ technique.

The Al alloy ingot were cut into small pieces and charged into the high-temperature muffle furnace in a graphite crucible. In the other furnace, the inorganic powders were preheated at the 250 °C. When the temperature of the Al alloy reached 850 °C, preheated inorganic powders were charged into the Al alloy melt and mixed with the help of mechanical stirrer of graphite. The temperature of the melt was maintained at 850 °C during the stirring and it was frequently checked by the external K-type thermocouple. The mechanical stirring was done up to 30 min. The molten Al alloy reacted with the inorganic powders and formed the reinforcement particles. Finally, the melt was degassed using the hexa-chloro-ethane and solidified into the permanent mould using bottom pouring cantilever arrangement. The casting size was 2 cm × 2 cm × 15 cm. With the above fabrication procedure, four compositions with 10 vol% Al_3Zr particles and varying amounts of ZrB_2 particles (0, 1, 3 and 5 vol%) were prepared and designated as C1, C2, C3 and C4, respectively. The required amount of the K_2ZrF_6 salt was 151 g, 185 g, 253 g and 322 g, while KBF_4 salt was 0 g, 30 g, 91 g and 152 g for the C1, C2, C3 and C4 composite, respectively. The composites were fabricated up to the 5 vol% of ZrB_2 particles because beyond this vol% of particles, the fluidity of the melt was decreased and the melt became highly viscous with poor castability.

The different phases, morphologies and the distributions of particles in the composites were identified using elemental analysis through energy-dispersive spectroscopy (EDS) and scanning electron microscope (ESEM Quanta 200FEG).

2.2 Tribological characterization and worn surface studies

Four compositions of the composites with varying vol% of ZrB_2 were studied for the tribological properties. Wear and friction studies under dry sliding conditions were conducted on pin-on-disc configuration of a multi-function tribometer

from Rtec Instruments, USA. Experiments were performed in opposition to steel disc with hardness of 62 HRc at different operating conditions of normal load sliding distance and sliding velocity. Cylindrical specimens according to ASTM standards were used for friction and wear tests. Before wear test, the surfaces of the specimen and disc were polished and washed by acetone. Each one of the experiments was carried out at ambient temperature under dry condition. The experiments were conducted for normal load (10–40 N), sliding distance (300–3000 m) and sliding velocity (1–4 m/s) for all composites. Surface roughness was maintained at ≤ 0.39 µm for the cylindrical pin specimens and counterpart steel disc with conformal contact. The conformal means the nominal contact area during the wear testing which remains approximately constant. The values of wear rate were calculated from the dividing of volume loss by sliding distance. Volume loss is calculated by the following formula [ASTM-G99-05]

$$\text{volume loss} = \frac{\text{loss in mass}}{\text{density}} \times 1000 \tag{1}$$

Volume loss, mass loss and density are in mm^3, g and g/cm^3, respectively. Three values for each data point have been taken and averaged out to draw the figures. The standard deviation has been calculated and shown in respective figures.

The friction coefficient was measured by dividing recorded friction force by respective load, and the average value was reported. Pin-on-disc apparatus and specimen are shown in Fig. 1 schematically. However, pin-on-disc (POD) configuration of a multi-function tribometer with different components is shown in Fig. 2. To understand the mechanism and intensity of damage after wear test, the surface texture was studied under EDS attached to the FESEM Quanta 200FEG SEM and also under 3D-profilometer from Rtec Instruments.

2.3 Coefficient of thermal expansion

Coefficient of linear thermal expansion for all compositions was evaluated in a temperature range of RT to 373 K (100 °C) using Turner's model [4]

$$\alpha_c = \frac{V_r K_r \alpha_r + V_m K_m \alpha_m}{V_r K_r + V_m K_m} \tag{2}$$

where α_c, V, K, r and m are coefficient of thermal expansion for composite, volume fraction, bulk modulus, reinforcement phase and matrix phase, respectively. The values of coefficient of thermal expansion for ZrB_2, Al_3Zr and base alloy are $6.88\times10^{-6}\ K^{-1}$, $12.60\times10^{-6}\ K^{-1}$ and $23.80\times10^{-6}\ K^{-1}$, respectively, while bulk modulus are 240 GPa, 100.05 GPa and 70.70 GPa, respectively [18–20]. These values were used to evaluate the coefficient of linear thermal expansion for all the compositions.

3 Results and discussion

3.1 Microstructural and phase's analysis

The SEM micrographs of composites with different vol% of ZrB_2 particles are shown in Fig. 3. The micrograph of C1 composite consists of Al alloy matrix and the Al_3Zr particles (Fig. 3a). These particles having the size range of 6–29 µm are homogeneously distributed with the polyhedron and rectangular morphology. The micrographs of C2–C4 composites consist of Al alloy matrix, Al_3Zr coarse particles and ZrB_2 particles clusters (Figs. 3b–d). The size of the ZrB_2 particles clusters increases with an increasing amount of ZrB_2 particles in the composites. The EDS analysis of ZrB_2 particles cluster, Al_3Zr particle is shown in Fig. 4a, b which confirms the successful formation of ZrB_2 and Al_3Zr

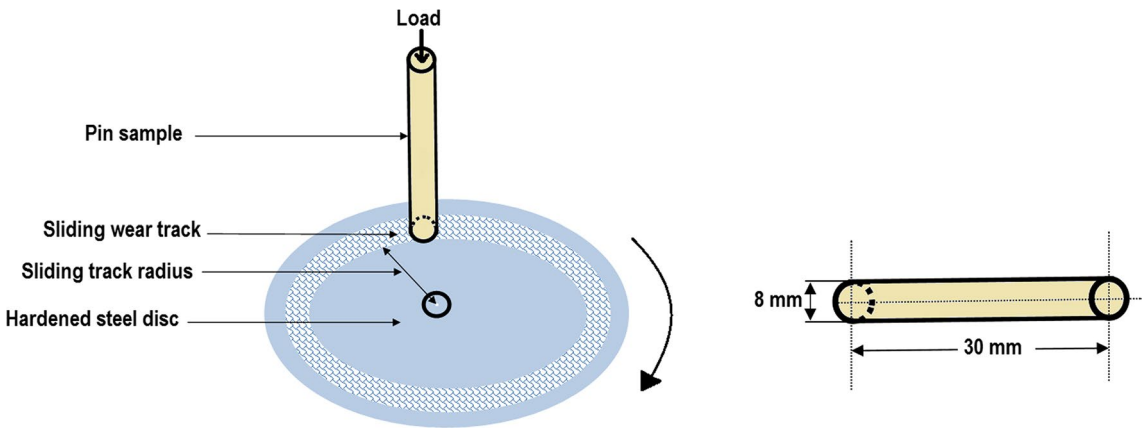

Fig. 1 Schematic diagram of pin-on-disc apparatus and specimen

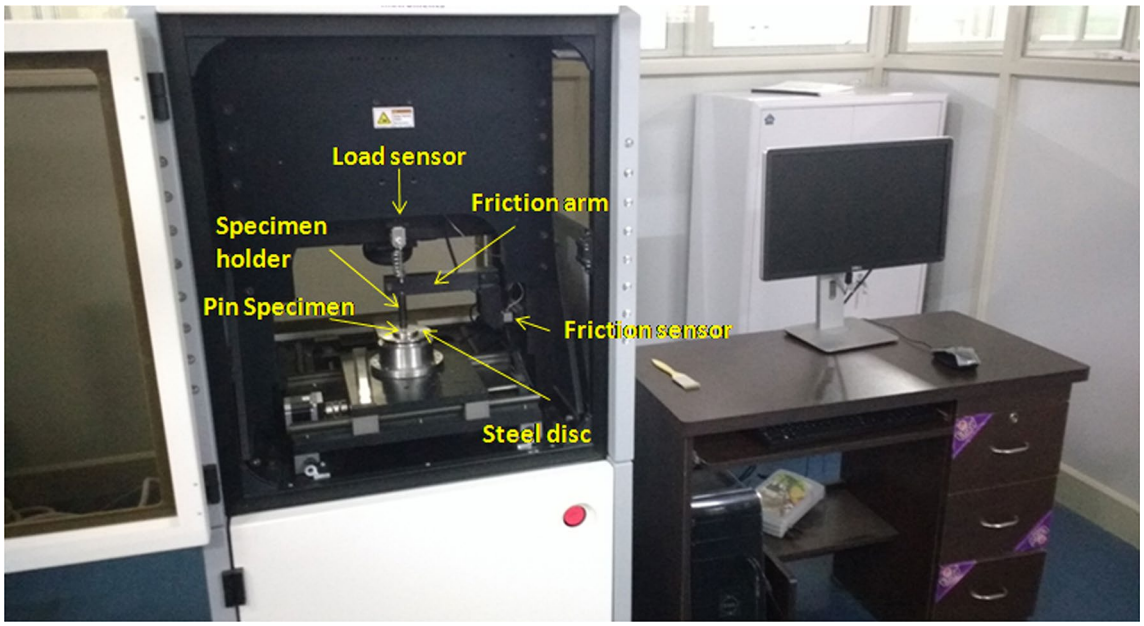

Fig. 2 Pin-on-disc (POD) configuration of a multi-function tribometer

particles in the composites. However, the SEM micrographs of the ZrB_2 particles at the higher magnification are shown in Fig. 4c, d, which clearly display that the ZrB_2 particles present in the morphology of hexagonal and rectangular within a size range of 10–190 nm.

3.2 Wear behaviour

3.2.1 Effect of sliding distance

The calculated cumulative mass loss with varying sliding distances for C1 to C4 composites under operating condition 20 N and 1 m/s is shown in Fig. 5. This figure illustrates that there is almost linear dependence between cumulative mass loss and sliding distance for all the composites which explains that there is only steady-state wear. The values of cumulative mass loss for the composites namely C1, C2, C3 and C4 are found as 0.02 g, 0.017 g, 0.013 g and 0.009 g, respectively, after the 3000 m sliding distance at the constant sliding velocity (1 m/s) and normal load (20 N). Minimum cumulative mass loss is observed for C4 composite. Similar kind of trend between the cumulative mass loss and the sliding distance is also observed in the trialuminide-reinforced aluminium matrix composites [2].

3.2.2 Effect of normal load

The calculated wear rate and wear rate per unit vol% of reinforcement with varying loads for all the composites at 1 m/s are shown in Figs. 6a, b. Wear rate per unit vol% of reinforcement gives a measure of load-bearing capacity with increasing hard particles. It is observed that both wear parameters continuously increase with the increase in normal load for all composites. However, at all normal load, the minimum value of wear rate and wear rate per unit vol% of reinforcement is observed for the C4 composite. Analogous trend is depicted by ZrB_2-reinforced aluminium matrix composites as observed by Kumar et al. [21].

3.2.3 Effect of sliding velocity

The calculated wear rate and wear coefficient under varying sliding velocities for the composites at 20 N are shown in Fig. 7a, b. Wear coefficient is the load-bearing capacity. It is observed that wear rate of C2, C3 and C4 composites shows entirely different nature than C1 (without ZrB_2). For C1, wear rate initially decreases, but beyond 2.5 m/s, it increases sharply [19].

On the other hand, wear rate for C2, C3 and C4 composites increases slightly up to 2 m/s, but later a marginal decrease in wear rate is observed (Fig. 7a). It is interesting to note that the hybrid composites show much lower wear rate than C1 at high sliding velocity. Wear coefficient also shows the same nature which is shown in Fig. 7b. However, the minimum value of wear rate and wear coefficient is observed for the C4 composite at all sliding velocity. These figures indicate that hybrid composites can be successfully used at higher velocities.

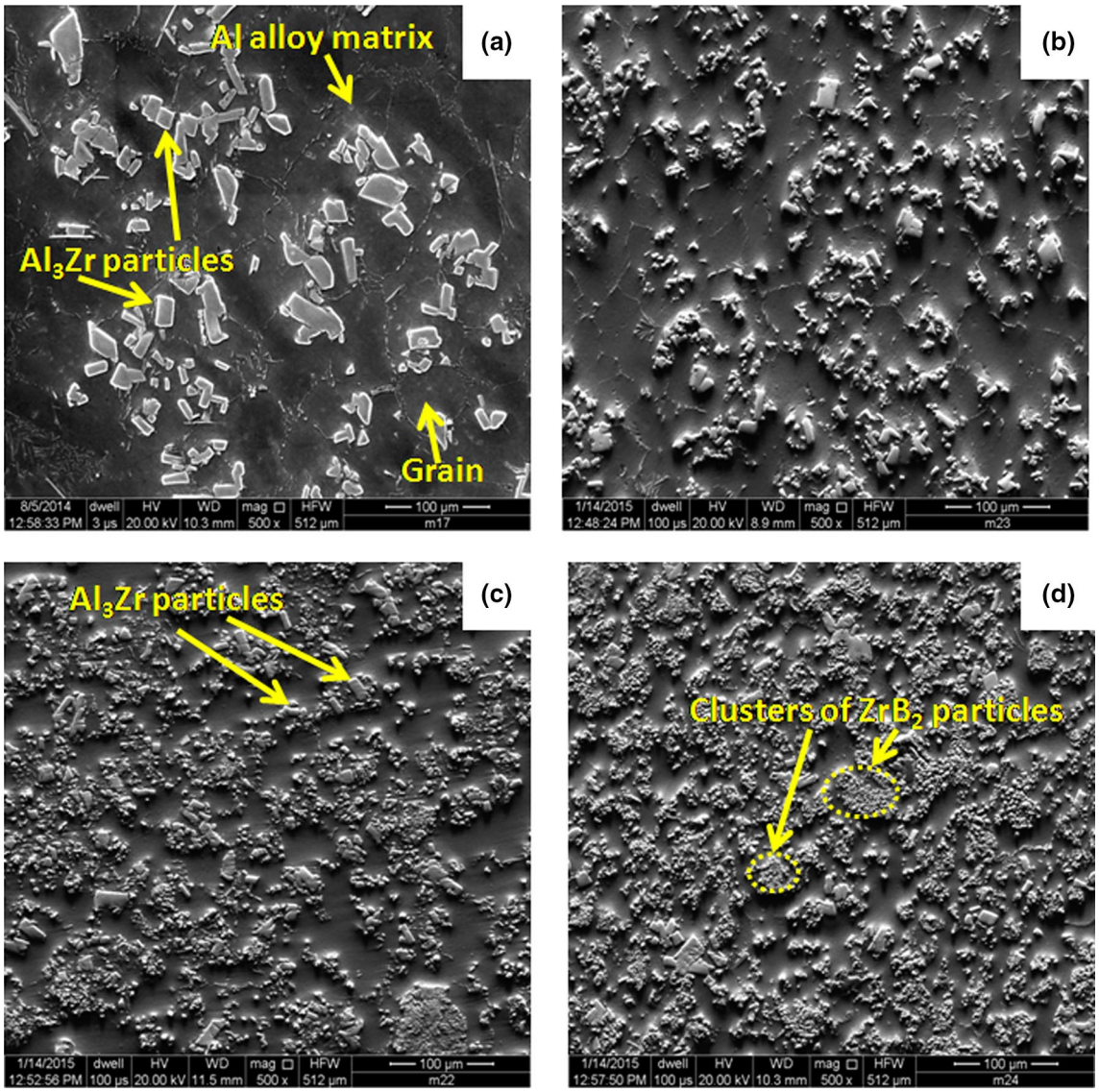

Fig. 3 SEM micrographs of composites with different vol% of ZrB_2 particles in C1 (**a**), C2 (**b**), C3 (**c**) C4 (**d**) [12]

3.2.4 Effect of compositions

The calculated wear rate and wear coefficient of all composites, i.e. C1, C2, C3 and C4, under operating condition 20 N and 1 m/s are shown in Fig. 8a, b. These figures clearly show that both wear parameters decrease with increasing vol% of ZrB_2. The minimum value of wear rate and wear coefficient is observed for the C4 composite. Gautam et al. [19] have also depicted the same observation on wear rate with composition in the aluminium matrix composites reinforced with the trialuminide particles.

3.3 Friction behaviour

3.3.1 Effect of sliding distance

The calculated COF with varying sliding distances for all composites under operating condition 20 N and 1 m/s is shown in Fig. 9. It is observed that friction coefficient fluctuates with sliding distance for all composites. However, the value at which the friction coefficient fluctuated increases with increasing vol% of ZrB_2 particles in the composites as also shown in Fig. 6. Mohan et al. [22] also

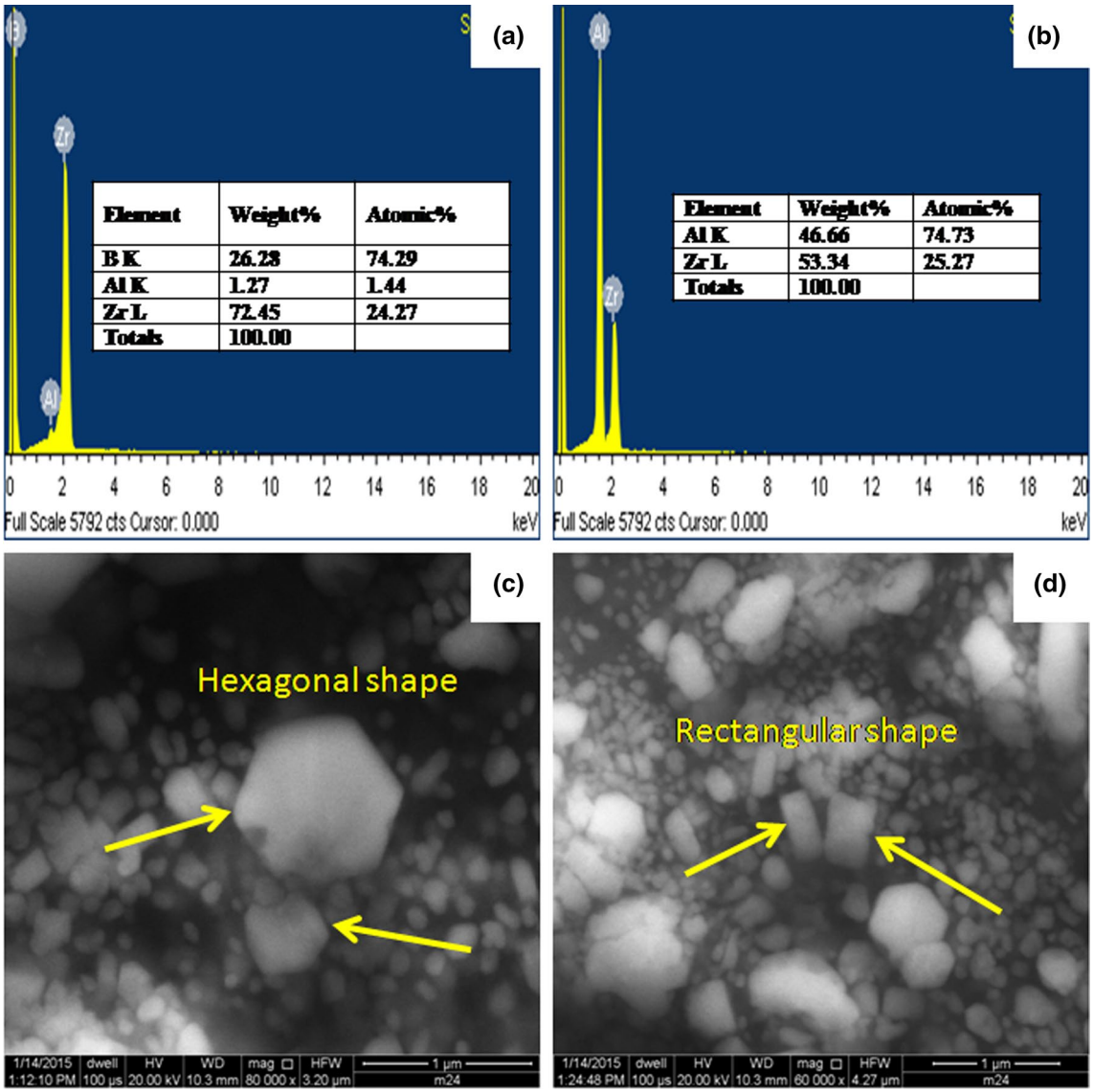

Fig. 4 EDS analysis of ZrB_2 particle (**a**); EDS analysis of Al_3Zr particle (**b**); morphology of ZrB_2 particles (**c**, **d**) [12]

reported the fluctuating behaviour in friction coefficient with sliding distance in the aluminium matrix composites.

3.3.2 Effect of normal load

The calculated COF with varying loads for all the composites at 1 m/s is shown in Fig. 10. It is found that coefficient of friction decreases continuously with load for all composites. However, among all the composites, C4 composite shows the maximum COF at all normal loads.

3.3.3 Effect of sliding velocity

The calculated COF with varying sliding velocities for all composites under 20 N is shown in Fig. 11. It is observed that coefficient of friction for C1 increases continuously with sliding velocity, whereas for hybrid composites (C2, C3 and C4) the COF shows a decreasing tendency up to 2 m/s, and thereafter, it increases for all hybrid composites. The hybrid composites follow the same trend in the COF vs sliding velocity as observed by Kumar et al. [21] in the ceramic-reinforced aluminium matrix composites under dry sliding wear.

3.3.4 Effect of compositions

The calculated COF with varying compositions under operating condition 1 m/s and 20 N is shown in Fig. 12. With increasing vol% of ZrB_2 particles, the friction coefficient is found to increase. However, the increasing rate of friction

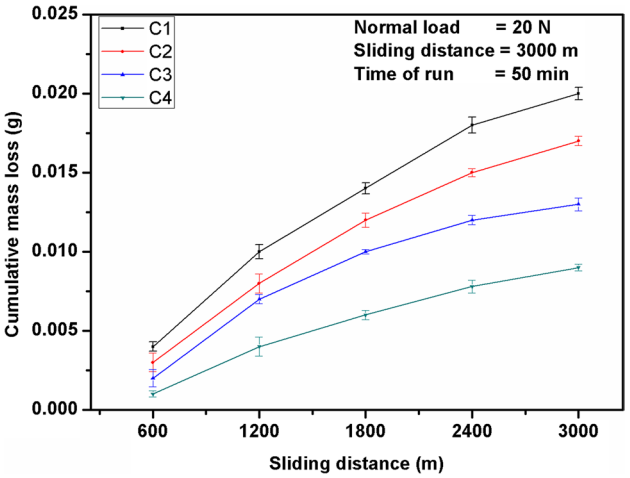

Fig. 5 Calculated cumulative mass loss under varying sliding distances

coefficient is different for different composites. Maximum increasing rate is observed for the C4 composite. Kumar et al. [21] have also described that the friction coefficient of aluminium matrix composite decreases with an increasing amount of ceramic reinforcement.

3.4 Coefficients of thermal expansion

The coefficients of thermal expansion are an important parameter in high-temperature applications where dimensional tolerance becomes important. The coefficient of linear and volumetric thermal expansion is represented by α_L and α_V for the composites, and their values are given in Table 1. The values of α_L are evaluated by Eq. (2) using the coefficient of thermal expansion, volume fraction, bulk modulus of reinforcement phases and matrix phase which has been mentioned in Sect. 2.3. However, the values of

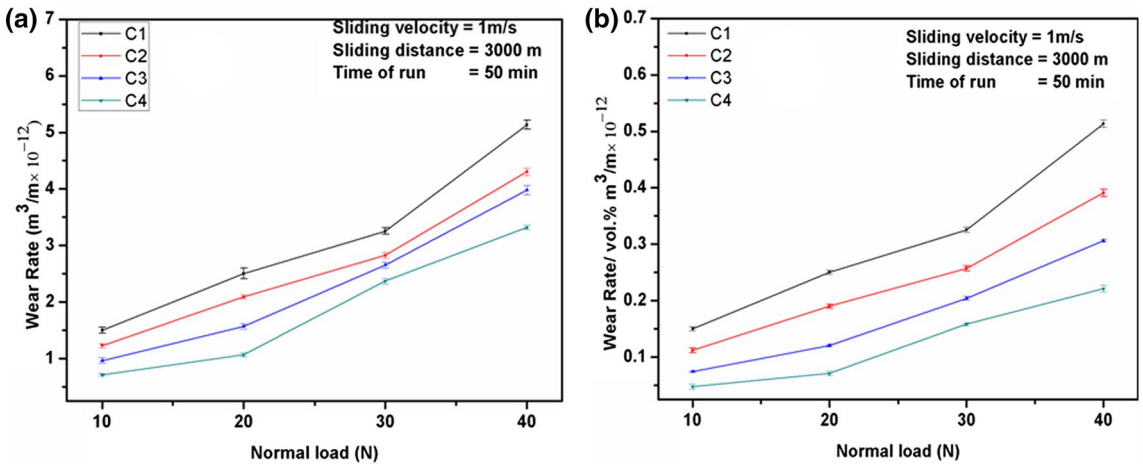

Fig. 6 Calculated wear rate (**a**) and wear per unit vol% reinforcement (**b**) under varying loads

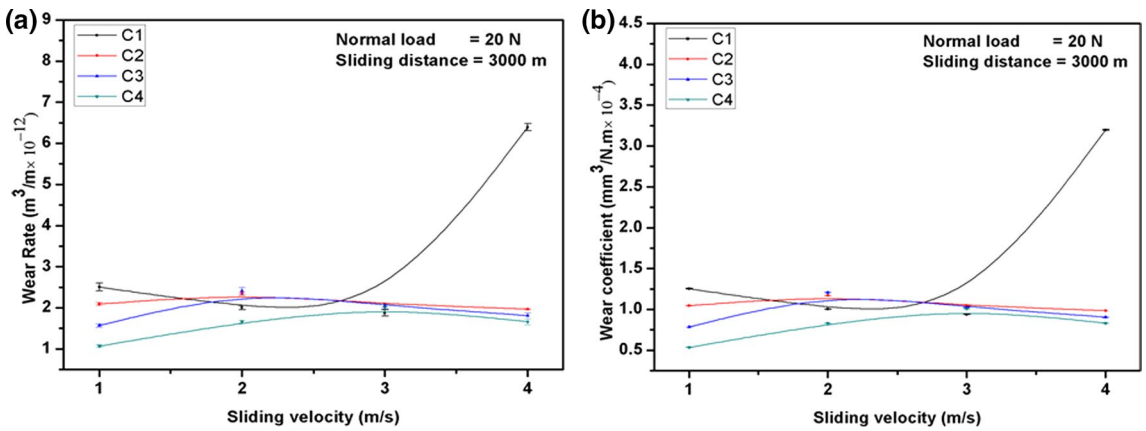

Fig. 7 Calculated wear rate (**a**) and wear coefficient (**b**) under varying sliding velocities

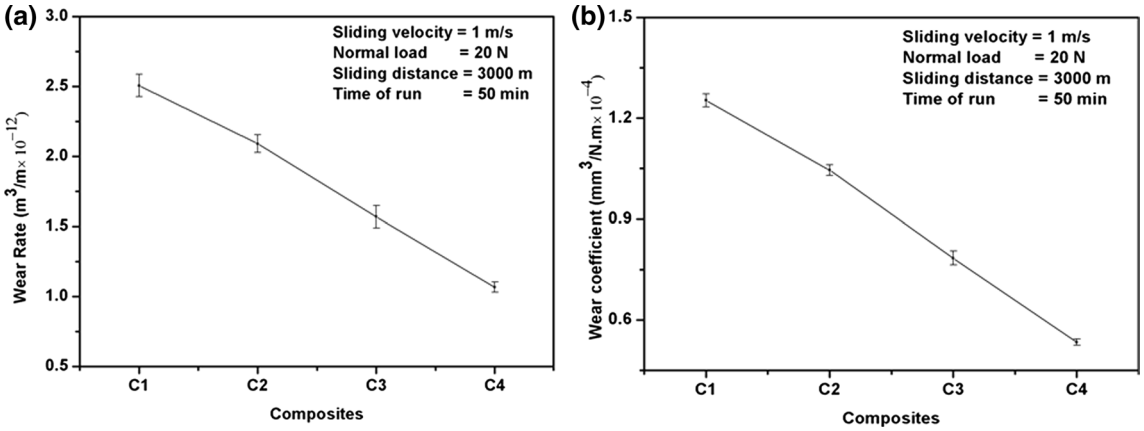

Fig. 8 Calculated wear rate (**a**) and wear coefficient (**b**) under varying compositions

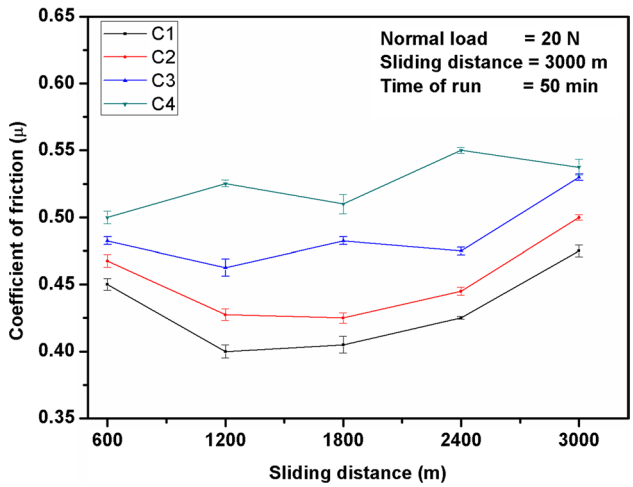

Fig. 9 Calculated COF under varying sliding distances

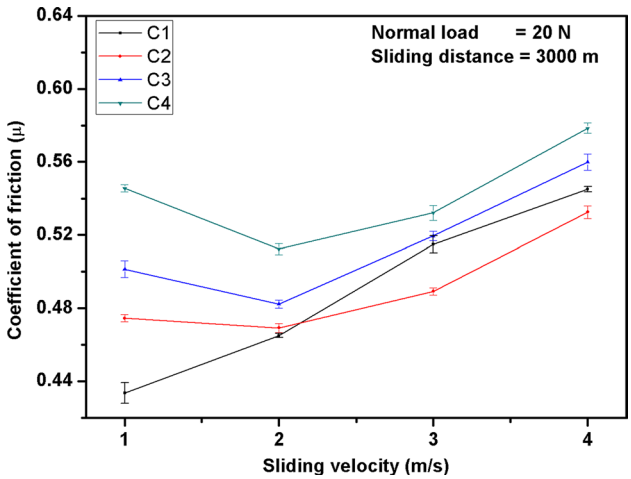

Fig. 11 Calculated COF under varying sliding velocities

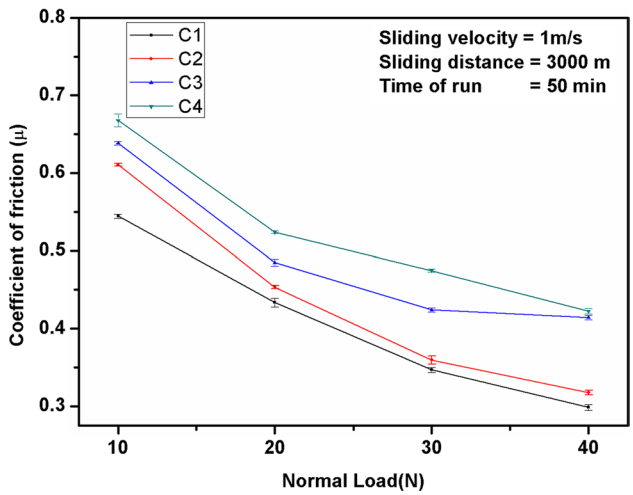

Fig. 10 Calculated COF under varying loads

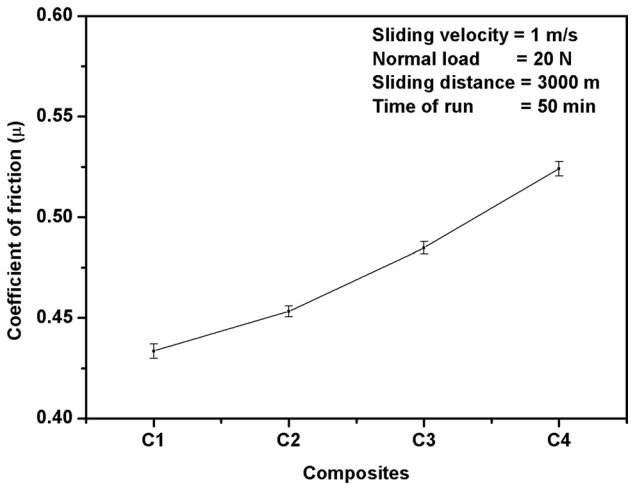

Fig. 12 Calculated COF under varying compositions

Table 1 Values of α_L and α_V for composites

S. no.	Materials designation	α_L ($\times 10^{-6}$ m/m K)	α_V ($\times 10^{-6}$ m/m K)
1	C1	22.21	66.63
2	C2	21.71	65.12
3	C3	20.77	62.30
4	C4	19.90	59.70

α_V are evaluated by the multiplication of α_L by a factor 3. Decreasing trend in CTE values is observed as the amount of ZrB_2 particles in the Al_3Zr/AA5052 composite increases. This seems to be due to low α of ZrB_2 phase as compared to Al_3Zr/AA5052 composite.

4 Wear surface texture and mechanism

Predicting wear and friction properties is not simple because it involves large number of parameters such as operating environment, operating conditions and material properties. Though it may not be possible to completely eliminate wear and friction under the given conditions, these can definitely be minimized by proper material choice and by studying post-test surface conditions of the material used. Surface conditions after test can help in deciding the further action to minimize wear and friction; further, it can also help to specify the range of parameters within which material can be used.

In the present study, ZrB_2 particles have been introduced in Al_3Zr/AA5052 composite by in situ reaction to see their effect on the various properties of the base composite. Figure 5 shows cumulative wear of composites with distance which is mostly linear in nature; however, some fluctuations in wear rate with distance are observed which could be due to the throwing out of hard particles from the surface and/or formation and breaking of oxide layer [23]. Coefficient of friction shows fluctuations within a range of ± 0.12 to ± 0.25 depending on the composition (Fig. 9). The fluctuation in the values could be due to the protruding of hard dispersed particles forthcoming in contact with steel disc causing coefficient of friction to increase [24].

Wear rate and wear per unit vol% reinforcement shows an increase within the experimental load range for all compositions (Fig. 6a, b). Wear rate increases with same rate up to 30 N, but beyond this load the wear rate increases sharply for C1 composite (without ZrB_2) which indicates the change in wear manner from mild to severe. Once ZrB_2 is introduced in composite, the sudden increase in wear rate is restricted and it varies with the same rate. With increasing amount of ZrB_2, the wear rate remains linear up to 40 N. This indicates that transition of wear from mild to severe is delayed on inclusion of ZrB_2, although wear rate increases with load. Texture studies show that deep craters are formed and deformation of the surface occurs with the increase in load as visible from 3D contours of profilometer (Fig. 13a, b). Subsequently the roughness values were found to be 2.23 µm and 4.17 µm at 30 N and 40 N load, respectively. Coefficient of friction shows completely reverse trend and it decreases with load. Though it seems unusual, high ductility of matrix material may entrap the hard particles, or particles may be ploughed away reducing the coefficient of fraction (Fig. 10).

Sliding velocity is another operating parameter which affects the wear rate and wear coefficient (Fig. 7a, b). Composite C1 (without ZrB_2) behaves in the same manner as any

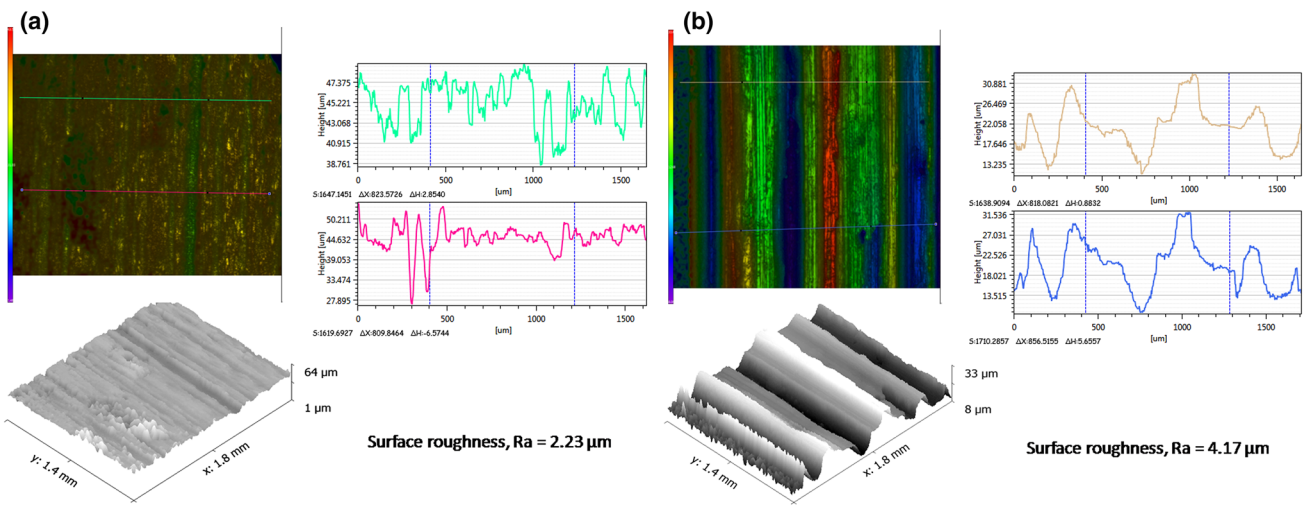

Fig. 13 2D and 3D surface profiles measured using profilometer of worn surface on different loads 30 N (**a**) and 40 N (**b**) for C4 composite at 1 m/s

other aluminium alloy or aluminium base composite in general [24, 25]. Both wear coefficient and wear rate decrease initially and attain a minimum value followed by a drastic increase in wear rate. But hybrid composites with ZrB_2 act differently. In these composites, initially a slight grow in wear is observed and it becomes almost stabilized with a marginal decreasing trend due to mild/oxidative wear of the surface (Fig. 14a). Here several phenomena take place simultaneously. With the increase in sliding velocity, asperities in the matrix are either chucked out or deformed and merged within the surface; oxidation of matrix becomes pronounced with the increase in temperature due to increased velocity; reinforced particles cause decrease in wear if entrapped within the surface or may lead to severe/oxidative-metallic wear if come out and act as third-body wear (Fig. 14b), and stress concentration fields are created due to large number of fine particles [23, 26].

In these hybrid composites, stress concentration takes place due to large number of particles that leads to crack nucleation which dominates in the initial stage over oxidation of the surface due to temperature rise [13, 27], as shown in Figs. 15a and b. But with the increase in velocity, oxide particles break and the rise in temperature softens the matrix phase. Al_3Zr, ZrB_2 and oxide particles instead of coming out of the surface to promote third-body wear are entrapped within the surface. However, nucleation and propagation of cracks still continue giving rise to surface roughness from 0.93 µm to 4.47 µm when sliding velocity increases from 2 m/s to 4 m/s (Fig. 16a, b) [28]. But the abundance of hard particles dominates the wear action and it is restricted to a lower wear rate (Fig. 7a). Wear coefficient also follows the same trend (Fig. 7b). Besides, originating of smooth oxide layer initially decreases the coefficient of friction, but with the increase in velocity the presence of large number of hard particles in the contacting surface rises the COF (Fig. 11) [13, 23]. Therefore, these in situ formed ($ZrB_2 + Al_3Zr$)/AA5052 hybrid composites could be a good candidate as wear resistant to friction material at high sliding velocity.

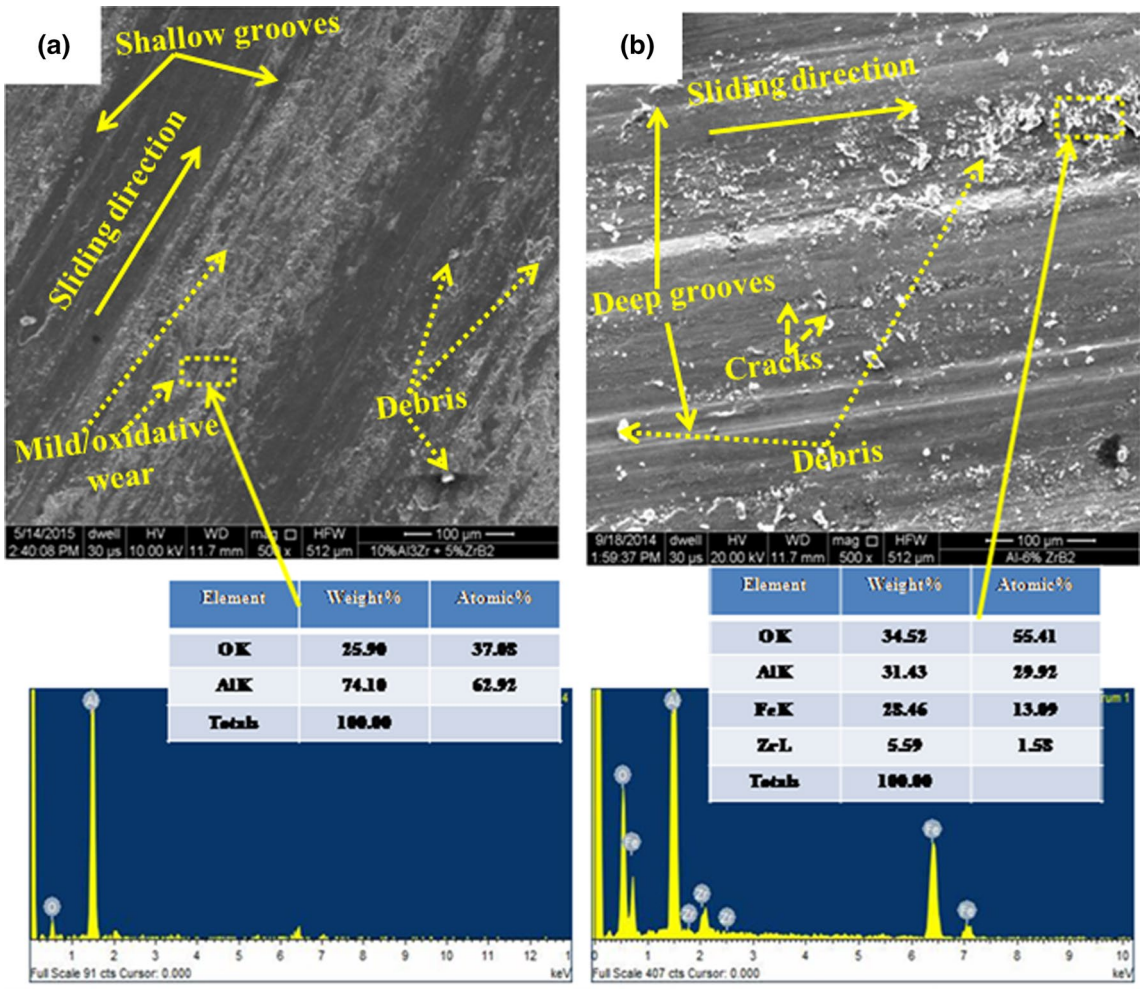

Fig. 14 SEM image with EDS analysis revealing the worn surface showing wear features include mild/oxidative (**a**) and severe/oxidative-metallic (**b**)

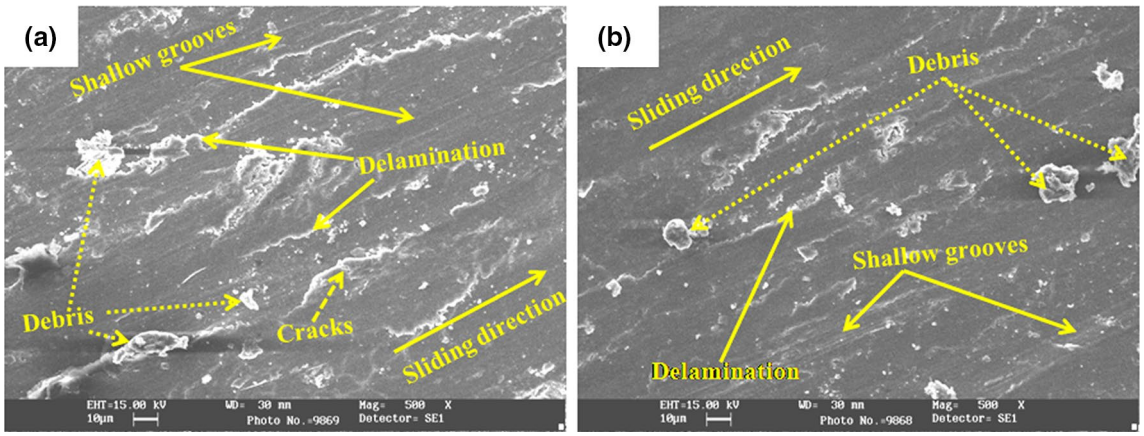

Fig. 15 SEM image revealing the worn surface of C3 (**a**) and C4 (**b**) at 20 N and 2 m/s

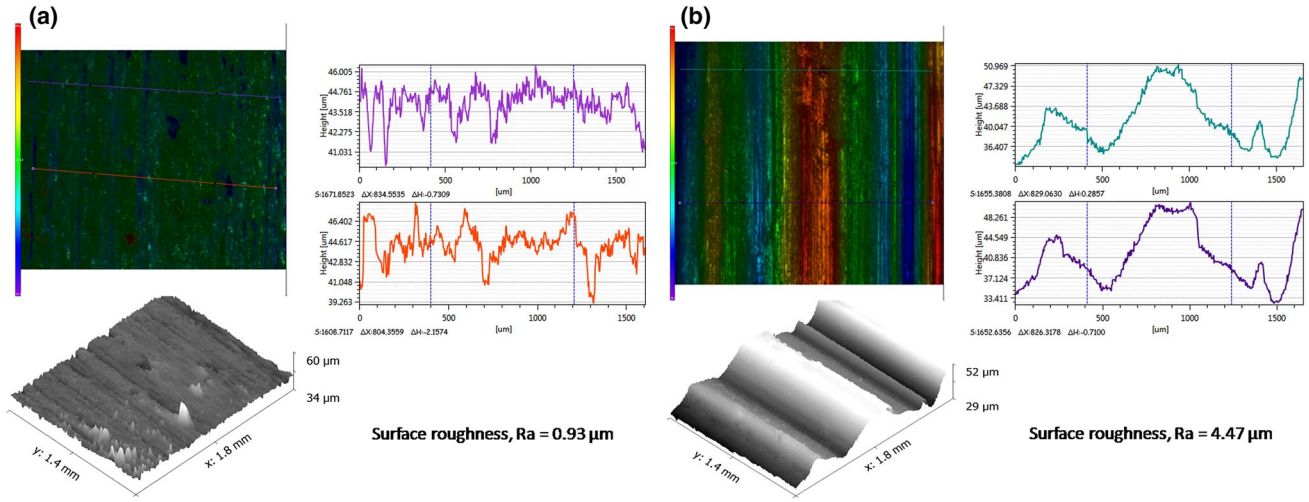

Fig. 16 2D and 3D surface profiles measured using profilometer of worn surface on different sliding velocities 2 m/s (**a**) and 4 m/s (**b**) for C4 composite at 20 N

With the addition/increase in the amount of ZrB_2 particles, both wear rate and wear coefficient decrease (Fig. 8a, b). In this case, again several factors contribute, but as operating parameters being the same, only stress concentration field leads to crack nucleation and propagation. The amount of hard particles is the controlling factor for wear rate. Though the surface gets distorted as evident from surface texture studies showing roughness contours (Fig. 17a–c), the level of distortion is less (Fig. 18a, b). The roughness values reduce from 1.82 to 1.40 µm due to the higher vol% of ZrB_2 particles which dominate the overall process causing both wear rate and wear coefficient to decrease. But COF being dominated by amount of hard particles increases continuously (Fig. 12).

5 Conclusions

- Wear rate with load studies shows that with the addition of ZrB_2 particles in Al_3Zr/AA5052 composites enable them for use up to a higher load while being in mild wear regime. The working load range improves with ZrB_2 particles.
- Wear rate and wear coefficient with sliding velocity can be reduced if ZrB_2 particles are incorporated in Al_3Zr/AA5052 composite, and they can be used successfully to a much higher velocity while being in mild wear regime only.
- The superior wear resistance and minimum wear rate are observed in the composite with 5 vol% of ZrB_2 particles, and the values are 0.937×10^{12} m/m^3 and

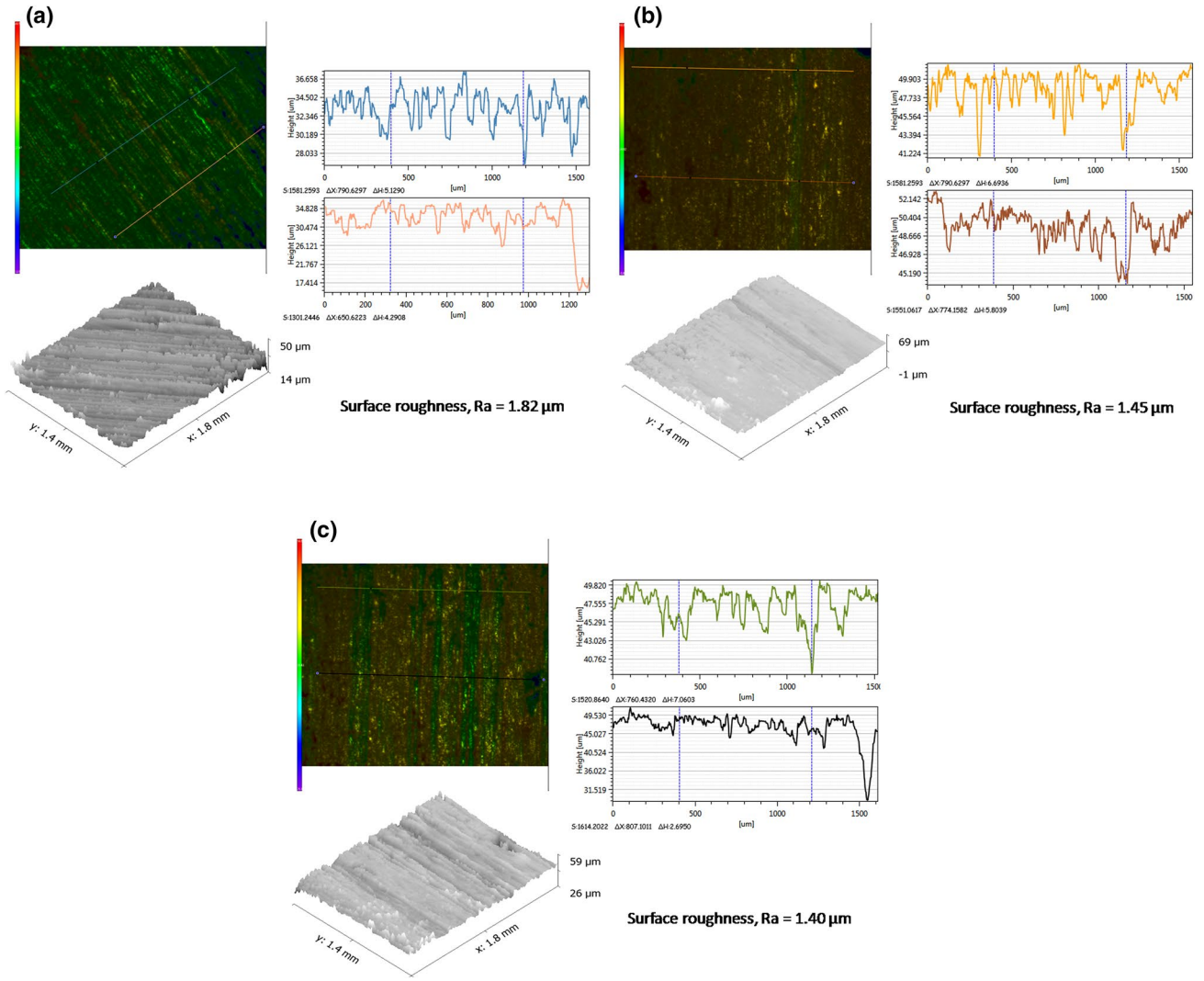

Fig. 17 2D and 3D surface profiles measured using profilometer of worn surface on different compositions C1 (**a**), C2 (**b**) and C3 (**c**) under operating condition 1 m/s and 20 N

1.067×10^{-12} m^3/m, respectively, at 20 N load and 1 m/s sliding velocity.

- Coefficient of friction (COF) shows a fluctuating tendency with sliding distance, while decreasing trend is observed with normal load.
- COF exhibits an increase trend with sliding velocity in composite (without ZrB_2), but for hybrid composites it shows a decreasing trend up to 2 m/s and beyond which it increases.
- The present investigation shows that in situ $(ZrB_2 + Al_3Zr)$/AA5052 hybrid composites could be a promising material in the applications requiring high wear resistance and high COF such as braking system.

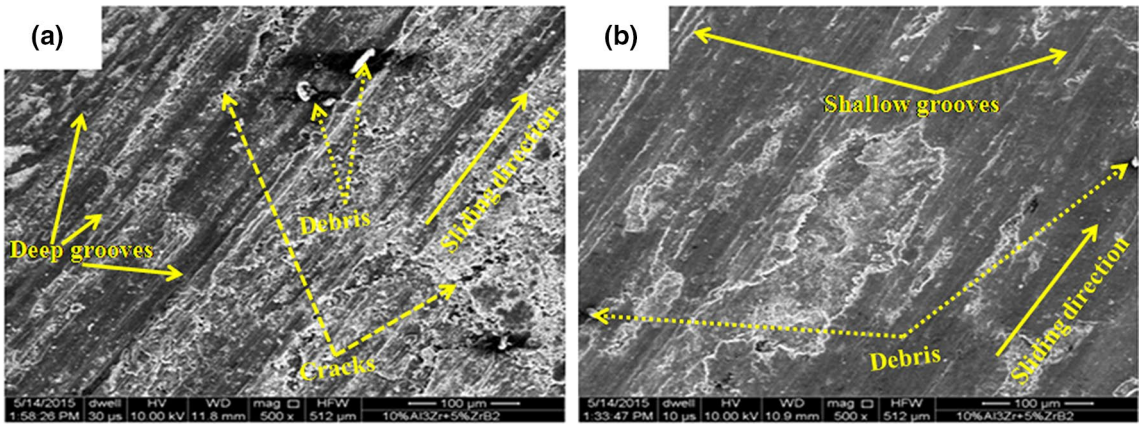

Fig. 18 SEM image revealing the worn surface showing wear features for C1 (**a**) and C2 (**b**) at 40 N

Acknowledgements The corresponding author acknowledges the Department of Science and Technology, India, for financial support under the SERB National Post-Doctoral fellowship scheme reference PDF/2016/002483.

References

1. Singh G, Chan LSI, Sharma N (2018) Parametric study on the dry sliding wear behaviour of AA6082–T6/TiB_2 in situ composites using response surface methodology. J Braz Soc Mech Sci 40(310):1–12
2. Gautam G, Mohan A (2015) Wear and friction of AA5052-Al_3Zr in situ composites synthesized by direct melt reaction. J Tribol 138:021602-1–021602-12
3. Kumar N, Gautam G, Gautam RK, Mohan A, Mohan S (2017) High-temperature tribology of AA5052/ZrB_2 PAMCs. J Tribol 139:011601-1–011601-12
4. Agarwal R, Mohan A, Mohan S, Gautam RK (2014) Synthesis and characterization of Al/Al_3 Fe nanocomposite for tribological applications. J Tribol 136:012001-1–012001-9
5. Singh R, Shadab M, Dash A, Rai RN (2019) Characterization of dry sliding wear mechanisms of AA5083/B_4C metal matrix composite. J Braz Soc Mech Sci 41(98):1–11
6. Stojanovic B, Vencl A, Bobic I, Miladinovic S, Skerlic J (2018) Experimental optimisation of the tribological behaviour of Al/SiC/Gr hybrid composites based on Taguchi's method and artificial neural network. J Braz Soc Mech Sci 40(311):1–14
7. Hynes NRJ, Sankaranarayanan R, Tharmaraj R, Pruncu CI, Dispinar D (2019) A comparative study of the mechanical and tribological behaviours of different aluminium matrix–eramic composites. J Braz Soc Mech Sci 41(330):1–12
8. Gautam G, Ghose AK, Chakrabarty I (2015) Tensile and dry sliding wear behavior of in-situ $Al_3Zr + Al_2O_3$-reinforced aluminum metal matrix composites. Metall Mater Trans A 46A:5952–5961
9. Dwivedi SP, Sharma S, Mishra RK (2015) Microstructure and mechanical behavior of A356/SiC/Fly-ash hybrid composites produced by electromagnetic stir casting. J Braz Soc Mech Sci 37:57–67
10. Zhang S, Zhao Y, Chen G, Cheng X (2007) Microstructures and dry sliding wear properties of in situ ($Al_3Zr + ZrB_2$)/Al composites. J Mater Process Technol 184:201–208
11. Zhao Y, Zhang S, Chen G, Cheng X (2007) Effects of molten temperature on the morphologies of in situ Al_3Zr and ZrB_2 particles and wear properties of ($Al_3Zr + ZrB_2$)/Al composites. Mater Sci Eng A 457:156–161
12. Gautam G, Mohan A (2015) Effect of ZrB_2 particles on the microstructure and mechanical properties of hybrid ($ZrB_2 + Al_3Zr$)/AA5052 in situ composites. J Alloys Compd 649:174–183
13. Mohan S, Srivastava S (2006) Surface behaviour of as-Cast Al–Fe intermetallic composites. Tribol Lett 22:45–51
14. Srivastava S, Mohan S (2011) Study of wear and friction of Al–Fe metal matrix composite produced by liquid metallurgical method. Tribol Ind 33:128–137
15. Dinaharan I, Murugan N, Parameswaran S (2011) Influence of in situ formed ZrB_2 particles on microstructure and mechanical properties of AA6061 metal matrix composites. Mater Sci Eng A528:5733–5740
16. Gautam G, Kumar N, Mohan A, Gautam RK, Mohan S (2016) Influence of in situ formed ZrB_2 particles on microstructure and mechanical properties of AA6061 metal matrix composites. J Compos Mater 50:4123–4133
17. Gautam G, Kumar N, Mohan A, Gautam RK, Mohan S (2016) High-temperature tensile and tribological behavior of hybrid ($ZrB_2 + Al_3Zr$)/AA5052 in situ composite. Metall Mater Trans A47:4709–4720
18. Tian K, Zhao Y, Jiao L, Zhang S, Zhang Z, Wu X (2014) Effects of in situ generated ZrB_2 nano-particles on microstructure and tensile properties of 2024Al matrix composites. J Alloys Compd 594:1–6
19. Gautam G, Kumar N, Mohan A, Gautam RK, Mohan S (2016) Synthesis and characterization of tri-aluminide in situ composites. J Mater Sci 51:8055–8074
20. Okamoto NK, Kusakari M, Tanaka K, Inui H, Yamaguchi M, Otani S (2003) Temperature dependence of thermal expansion and elastic constants of single crystals of ZrB_2 and the suitability of ZrB_2 as a substrate for GaN film. J Appl Phys 93:88–93
21. Kumar N, Gautam G, Gautam RK, Mohan A, Mohan S (2016) Wear, friction and profilometer studies of in situ AA5052/ZrB_2 composites. Tribol Int 97:313–326

22. Mohan A, Gautam G, Kumar N, Mohan S, Gautam RK (2016) Synthesis and tribological properties of AA5052-base in situ composites. Compos Interface 23:503–518
23. Bhushan B (1999) Principles and applications of tribology. Wiley, New York
24. Mohan S, Pathak JP, Gupta RC, Srivastava S (2002) Wear behaviour of graphitic aluminium composite sliding under dry conditions. Int J Mater Res 93:1245–1251
25. Pathak JP, Mohan S (2005) Wear of conventional and experimental aluminium bearing alloys sliding under lubrication. Int J Mater Res 96:297–303
26. Mohan S, Mohan A (2015) Wear, friction and prevention of tribosurfaces by coatings/nanocoatings. In: Aliofkhazraei M (ed) Anti-abrasive nanocoatings: current and future applications. Elsevier, New York
27. Mandal D, Dutta BK, Panigrahi SC (2008) Effect of wt% reinforcement on microstructure and mechanical properties of Al-Mg base short steel fiber composites. J Mater Process Technol 198:195–201
28. Gautam G, Kumar N, Mohan A, Gautam RK, Mohan S (2016) Tribology and surface topography of tri-aluminide reinforced composites. Tribol Int 97:49–58